

Distributed Feedback Optimisation for Robotic Coordination

Antonio Terpin, Sylvain Fricker, Michel Perez

ETH Zürich

Zürich, Switzerland

aterpin@ethz.ch, frickers@ethz.ch, miperez@ethz.ch

Abstract—Feedback optimisation is an emerging technique aimed at steering a system to an optimal steady state for a given objective function. We show that it is possible to employ this control strategy in a distributed manner to coordinate a swarm of agents for moving in formation towards a target. Moreover, we prove that the asymptotic convergence to the set of optimal configurations is guaranteed. Finally, we analyse the topological structure of the specified formation to derive sufficient conditions on the convergence of the swarm in formation around the desired target location.

I. INTRODUCTION

Feedback optimisation is an emerging technique aimed at steering a system to a trajectory computed online that is optimal with respect to a selected objective function, relying on little information on the controlled plant. In particular, we consider the problem of driving a swarm of agents in formation towards the desired area using a distributed feedback optimisation approach. The formation specification (i.e., the desired inter-agents relative positions) as well as the target location fully describe such a task.

A thorough review on the feedback optimisation methodology can be found in [1], where the prototypical problem setup is presented, and compared to other existing optimisation-driven approaches. Remarkably, the plant dynamics need not be known. Instead, this approach relies only on the knowledge of the steady-state input-output sensitivity. As a result, feedback optimisation lessens the errors due to model mismatch and unmodelled disturbances. A classical example is congestion control for cyber-networks, where source controllers and link dynamics are the modelled feedback loop. In [2] such a problem is formulated as a projected saddle-flow dynamics, and the control law employed by the sources relies only on local information. A field of application of feedback optimisation that gained traction in recent years is power systems. A detailed overview on this topic can be found in [3], where a particular emphasis is put on the analysis of distributed systems and optimisation algorithms. The recent experimental validation obtained on power grids [4] empirically shows the promises of this approach. This naturally motivates investigating further application domains where feedback optimisation can be applied. Moreover, the recent work on saddle-flow dynamics for constrained convex optimisation problems on linear time-invariant systems [5], even in a time-varying, possibly non-regular domain [6] open the possibilities for further work on more complex tasks, also in the context of robotics coordination. For instance,

projected-flow dynamics could be employed to enforce environmental constraints.

Most of the work on robotics coordination for flocking is inspired by the so-called Reynolds principles [7], and typically employs the concept of potential forces. An influential work in this context is [8], where the author presents a general framework for distributed flocking algorithms. The main difference is that in our work, we use potential-like functions within the framework of feedback optimisation and thus, the control scheme relies only on the steady-state input-output map of the plant, rather than on low-level knowledge. Notably, along the lines of closed-loop optimisation for robotics coordination, feedback optimisation is used in [9] to learn generalised Nash Equilibrium in a non-cooperative game-theoretical setting. The procedure relies on iteratively applying best-response strategies. However, this requires information on the whole swarm. To the best of our knowledge, this paper is the first work that uses feedback optimisation for robotics coordination in a distributed manner. Our theoretical analysis on the asymptotic convergence of the closed-loop system builds on [10], where the authors quantify the required timescale separation to ensure stability and convergence of the interconnection of an exponentially stable plant and different schemes of feedback optimisation.

In this paper, we tackle the robotics coordination problem through feedback optimisation. In particular, we show that it is possible to implement such a scheme in a distributed manner. Moreover, we prove the convergence of the swarm to the configuration that minimises the selected cost function. To this scope, we build on [10] to show that exponential stability is required only for the portion of the state that affects the considered output, whereas for the rest only asymptotic stability is necessary. Furthermore, we derive conditions on the cost function coefficients and topology of the formation graph. These guarantee that the optimal closed-loop steady-states for the given objective function are such that the agents asymptotically gather in formation around a target location.

The remainder of this paper is organised as follows. Section II introduces the problem and the control scheme we want to pursue. In Section III, we analyse the closed-loop system and we present the main results of our work. Section IV contains technical results that used along the way and Section V presents empirical results and concrete instances of the presented problem.

II. PROBLEM STATEMENT

The goal of this work is to drive a swarm of N agents into a given formation around a given target location. We consider unicycle dynamics for the generic i -th agent with state $x_i = [r_i^T, \theta_i]^T$, where $r_i = [a_i, b_i]^T$ is the position of the i -th agent in the $a-b$ plane and θ_i its orientation with respect to the a -axis. The dynamics are:

$$\dot{a}_i = v_i \cos(\theta_i), \quad \dot{b}_i = v_i \sin(\theta_i), \quad \dot{\theta}_i = \omega_i, \quad (1)$$

where the low-level control inputs v_i and ω_i are to be defined.

In particular, we design the actuation mechanism available on each agent to track a given fixed reference position p_i . Consider the error variables

$$\begin{aligned} \xi_{a_i} &= p_{a_i} - a_i, & \xi_{b_i} &= p_{b_i} - b_i, \\ \xi_i &= \sqrt{\xi_{a_i}^2 + \xi_{b_i}^2}, & \phi_i &= \text{atan2}(\xi_{b_i}, \xi_{a_i}) - \theta_i \end{aligned}$$

and the low-level control (llc) law

$$\begin{aligned} v_i &= k_i \xi_i \cos(\phi_i), \\ \omega_i &= k_i \left(\cos(\phi_i) \sin(\phi_i) + \frac{\sin(\phi_i)^2}{\phi_i} \right), \end{aligned} \quad (2)$$

continuously extended with $\omega_i = 0$ when $\phi_i = 0$, and $k_i > 0$.

Lemma II.1. *The low-level control law (2) stabilises (1). Moreover,*

- $\phi_i(t)^2 \leq \phi_i(t_0)^2 \iff |\phi_i(t)| \leq |\phi_i(t_0)|$,
- $|\phi_i(t_0)| < \pi/2 \Rightarrow \cos(\phi_i(t)) \geq \cos(\phi_i(t_0)), \phi_i(t) \rightarrow 0$
- $\xi_i(t) \leq \xi_i(t_0) \exp(-k_i t)$.

Proof. The proof is provided in subsection IV-A. \square

Every agent has access to its own global position and the relative positions of its neighbours specified through the undirected and unweighted formation graph $G = (\mathcal{V}, \mathcal{E})$, where the set of vertices \mathcal{V} consists of all N agents and the set of edges \mathcal{E} captures the connections between the agents. Without loss of generality, we can assume that each agent has access to $y_i = [r_i^T, [r_j^T]_{j \in \mathcal{N}(i)}]^T$, as every agent can calculate the absolute position of its neighbours $\mathcal{N}(i)$ knowing its own and their relative positions. Hence, the output map of each agent is $g_i(x_i) = r_i$, and the output of the whole swarm is the stacked positions of all the agents $r = [[r_i^T]_{i \in \mathcal{V}}]^T$, N being the number of robots. The steady-state input-output map of the swarm and its sensitivity are then (see derivation in subsection IV-C):

$$h(u) = u, \quad \mathbb{J}h(u) = I_{2N}, \quad (3)$$

where I_k is the $k \times k$ identity matrix and with \mathbb{J} we denote the Jacobian of the vector field. Recall that the steady-state input-output map is defined as $h(u) = \lim_{t \rightarrow \infty} g(x(t))$.

The target formation is specified by the relative positions between agents, d_{ij} for all $(i, j) \in \mathcal{E}$, where the direction is defined through the incidence matrix B (see example in Section V) with arbitrary orientation of the edges. We denote by $d = [[d_{ij}^T]_{(i,j) \in \mathcal{E}}]^T$ the stacked relative positions of the agents according to the ordering of the edges given by the

incidence matrix B . Namely, we want r such that $\forall (i, j) \in \mathcal{E}$ $r_i - r_j = d_{ij}$. For simplicity, we assume that an agent always has access to the relative position of the agents it is adjacent to in the formation, regardless of their current distance. The desired final location of the swarm, τ , is assumed to be known for all agents.

Assumption II.1. *The formation graph G is connected and the inter-agent relative positions d uniquely define the formation. That is, $\forall i \neq j \in \mathcal{V}$, $r_i - r_j$ is uniquely defined if $r_i - r_j = d_{ij} \forall (i, j) \in \mathcal{E}$.*

To achieve the desired task, we propose the cost function

$$\Phi(r) = \frac{\gamma_1}{2} \sum_{(i,j) \in \mathcal{E}} \|r_i - r_j - d_{ij}\|^2 \quad (4a)$$

$$+ \frac{\gamma_2}{2} \sum_{i \in \mathcal{V}} \|r_i - \tau\|^2, \quad (4b)$$

where $\gamma_1, \gamma_2 > 0$ denote the weights on the formation error and the distance from the target respectively. $\|\cdot\|$ denotes the euclidean norm. We manipulate the terms of the cost function to write it in matrix form.

$$\begin{aligned} (4a) &= \frac{\gamma_1}{2} \sum_{(i,j) \in \mathcal{E}} (r_i - r_j)^T (r_i - r_j) \\ &\quad - \gamma_1 \sum_{(i,j) \in \mathcal{E}} (r_i - r_j)^T d_{ij} + \text{const.} \\ &= \frac{\gamma_1}{2} [r^T (L_G \otimes I_2) r - 2d^T (B \otimes I_2)^T r] + \text{const.} \\ (4b) &= \frac{\gamma_2}{2} \sum_{i \in \mathcal{V}} (r_i^T r_i - 2\tau^T r_i) + \text{const.} \\ &= \frac{\gamma_2}{2} [r^T r - 2(\mathbf{1}_N \otimes \tau)^T r] + \text{const.}, \end{aligned}$$

where $L_G = BB^T$ is the Laplacian of the formation graph G and \otimes is the Kronecker product. Hence, the cost function can equivalently be expressed as

$$\begin{aligned} \Phi(r) &= \frac{\gamma_1}{2} [r^T (L_G \otimes I_2) r - 2d^T (B \otimes I_2)^T r] \\ &\quad + \frac{\gamma_2}{2} [r^T r - 2(\mathbf{1}_N \otimes \tau)^T r] + \text{const.} \end{aligned}$$

with gradient

$$\begin{aligned} \nabla \Phi(r) &= \gamma_1 [(L_G \otimes I_2) r - (B \otimes I_2) d] \\ &\quad + \gamma_2 [r - (\mathbf{1}_N \otimes \tau)]. \end{aligned} \quad (5)$$

The closed loop system is

$$\dot{x} = f(x, u) \quad (6a)$$

$$\dot{u} = -\epsilon \mathbb{J}h(u)^T \nabla \Phi(r), \quad (6b)$$

where (6a) is the plant dynamics comprising the low-level controller and (6b) is the feedback-optimisation control-law dynamics. Explicitly, we have

$$\begin{aligned} \dot{u} &= -\epsilon \gamma_1 [(L_G \otimes I_2) r - (B \otimes I_2) d] \\ &\quad - \epsilon \gamma_2 [r - (\mathbf{1}_N \otimes \tau)]. \end{aligned} \quad (7)$$

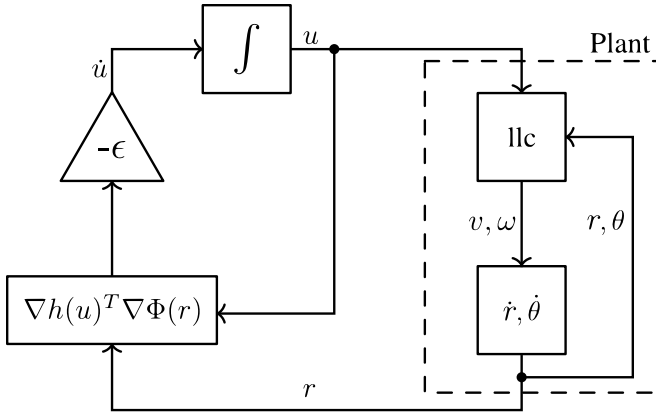


Fig. 1. Control scheme for the considered problem.

The scheme of such closed-loop system is shown in Figure 1. Notice that the integrator block in Figure 1 requires an initial condition for u_0 , which can be selected such that the angular error ϕ_i is arbitrarily small at the beginning for all agents. Therefore, the following assumption is not restrictive, and ensures that $|\phi_i(t)| < \pi/2$ and $\cos(\phi_i(t)) \geq \cos(\phi_i(t_0)) \forall i \in \mathcal{V}$ (Lemma II.1).

Assumption II.2. $|\phi_i(t_0)| < \pi/2 \forall i \in \mathcal{V}$.

III. CLOSED LOOP ANALYSIS

We now present the main results of this paper. Namely, we first show in subsection III-A that the resulting closed-loop control law is distributed. Then, in subsection III-B, we prove that the robotics swarm asymptotically converges and optimises the cost function (4). Finally, in subsection III-C we provide bounds on the gains related to the topological structure of the desired formation to guarantee that the optimal configurations with respect to the specified cost function correspond to the agents being in formation around the target location.

A. Feedback optimisation as a distributed control law

To show that the control-law in (6b) uses only local information for the i -th entry, we derive the input dynamics for the i -th agent:

$$\begin{aligned} \dot{u}_i = & -\epsilon\gamma_1 \sum_{j \in \mathcal{N}_B^o(i)} (r_i - r_j - d_{ij}) \\ & - \epsilon\gamma_1 \sum_{j \in \mathcal{N}_B^i(i)} (r_i - r_j + d_{ji}) \\ & - \epsilon\gamma_2(r_i - \tau), \end{aligned}$$

where the in and out neighbours (\mathcal{N}_B^i and \mathcal{N}_B^o respectively) are denoted with respect to the orientation of the graph provided by the incidence matrix.

It can be observed that the control law depends only on the local sensing $y_i = [r_i^T, [r_j^T]_{j \in \mathcal{N}(i)}]^T$. The scheme of the resulting distributed control law is shown in Figure 2.

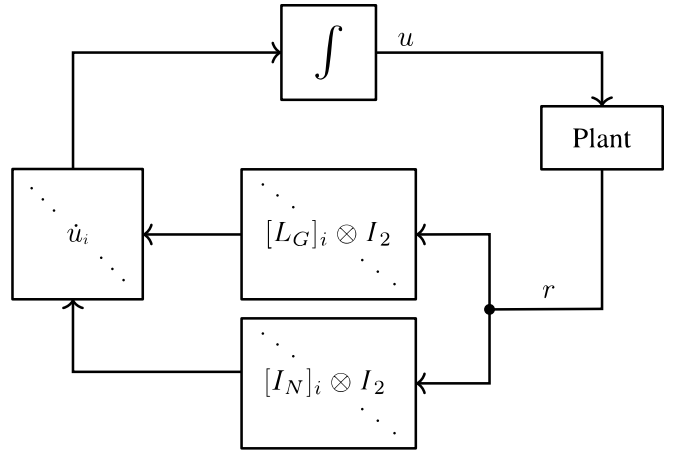


Fig. 2. Resulting distributed control scheme for the cost function in (4).

B. Asymptotic behaviour

The key motivation of this subsection is that even if both the plant (1,2) and the control input dynamics (6b) are asymptotically stable, there is no guarantee a priori that their interconnection is. Moreover, due to the lack of exponential stability of the entire state of the plant (1,2) [10, Theorem III.2] does not apply. Therefore, in the following we show that we only require exponential stability for the portion of the state that is actually measured in the output and affects the cost, as long as asymptotic stability of the system is given.

Assumption III.1. Let x be the state of the plant and $r = g(x)$ the measured part that appears in the cost function. Then, there exist a differentiable function $W(r, p) \geq 0$ and $\alpha, \beta, \gamma, \mu > 0$ such that:

- $\alpha \|r - h(p)\|^2 \leq W(r, p) \leq \beta \|r - h(p)\|^2$
- $\nabla_r W(r, p)^T \dot{r} \leq -\gamma \|r - h(p)\|^2$
- $\|\nabla_p W(r, p)\| \leq \mu \|r - h(p)\|$.

Further, we need the weakened Lipschitz condition in [10, Assumption III.1], and a Lipschitz condition on h .

Assumption III.2 ([10, Assumption III.1]). $\exists l > 0$ such that

$$\begin{aligned} \|\mathbb{J}h(u)^T [\nabla\Phi(r') - \nabla\Phi(r)]\| & \leq l \|r' - r\|, \\ \forall r', r, u \in \mathbb{R}^{2N}. \end{aligned}$$

Assumption III.3. h is q -Lipschitz continuous and $\text{null}[\mathbb{J}h(u)^T] = \{0_{2N}\}$.

We are now ready to state our variation of [10, Theorem III.2] that allows us to prove asymptotic convergence for our robotics swarm.

Theorem III.1. If Assumption III.1, Assumption III.2 and Assumption III.3 hold true, and the objective function (4) is differentiable with compact sub-level sets, the closed loop system (6) converges asymptotically to the set of critical points of (4) whenever $\epsilon < \sqrt{\frac{\gamma}{\mu l}}$.

Proof. We consider a LaSalle's function of the form

$$\begin{aligned}\Psi(x, u) &= (1 - \delta)\tilde{\Phi}(u) + \delta W(g(x), u), \\ \dot{\Psi}(x, u) &= (1 - \delta)\nabla\tilde{\Phi}(u)^T \dot{u} \\ &\quad + \delta \nabla_g W(g(x), u)^T \mathbb{J}g(x) \dot{x} \\ &\quad + \delta \nabla_u W(g(x), u)^T \dot{u}.\end{aligned}$$

where $\tilde{\Phi}(u) = \Phi(h(u))$ is the reduced cost (adopting the singular perturbation terminology).

The second term can be bounded as (Assumption III.1)

$$\nabla_g W(g(x), u)^T \mathbb{J}g(x) \dot{x} = \nabla_r W(r, u)^T \dot{r} \leq -\gamma \|r - h(u)\|^2,$$

whereas for the first and third term we can proceed as in the proof of [10, Lemma III.1].

Let $\kappa(x, u) = -\mathbb{J}h(u)^T \nabla\Phi(g(x)) = \dot{u}/\epsilon$. Then, for the first term we have

$$\begin{aligned}\nabla\tilde{\Phi}(u)^T \kappa(x, u) &= \nabla\Phi(h(u))^T \mathbb{J}h(u) \kappa(x, u) \\ &= (\nabla\Phi(h(u))^T - \nabla\Phi(g(x))^T) \mathbb{J}h(u) \kappa(x, u) \\ &\quad + \nabla\Phi(g(x))^T \mathbb{J}h(u) \kappa(x, u) \\ &\leq \|\mathbb{J}h(u)^T (\nabla\Phi(h(u)) - \nabla\Phi(g(x)))\| \|\kappa(x, u)\| \\ &\quad + \nabla\Phi(g(x))^T \mathbb{J}h(u) \kappa(x, u) \\ &\leq l \|h(u) - g(x)\| \|\kappa(x, u)\| \\ &\quad + \nabla\Phi(g(x))^T \mathbb{J}h(u) \kappa(x, u),\end{aligned}$$

where in the first inequality we used the Cauchy-Schwartz inequality [11, Theorem 7.1], and in the second we used Assumption III.2. Recalling the definition of κ , we finally obtain

$$\begin{aligned}\nabla\tilde{\Phi}(u)^T \kappa(x, u) \\ \leq l \|g(x) - h(u)\| \|\kappa(x, u)\| - \|\kappa(x, u)\|^2.\end{aligned}$$

For the third term we have (Assumption III.1)

$$\begin{aligned}\nabla_u W(g(x), u)^T \kappa(x, u) &\leq \|\nabla_u W(g(x), u)\| \|\kappa(x, u)\| \\ &\leq \mu \|r - h(u)\| \|\kappa(x, u)\|.\end{aligned}$$

Hence, since $g(x) = r$, we obtain

$$\begin{aligned}\dot{\Psi}(x, u) &\leq \left[\begin{array}{c} \|\kappa(x, u)\| \\ \|r - h(u)\| \end{array} \right]^T \Lambda \left[\begin{array}{c} \|\kappa(x, u)\| \\ \|r - h(u)\| \end{array} \right], \\ \Lambda &= \left[\begin{array}{cc} -(1 - \delta) & \frac{1}{2}(\epsilon l(1 - \delta) + \epsilon \mu \delta) \\ \frac{1}{2}(\epsilon l(1 - \delta) + \epsilon \mu \delta) & -\gamma \delta \end{array} \right],\end{aligned}\quad (8)$$

which is negative definite if ([12, pp.296])

$$\delta = \frac{l}{\mu + l} \text{ and } \epsilon < \sqrt{\frac{\gamma}{\mu l}}.$$

Moreover, we notice that the for the left hand side of (8) to be zero, we need the right hand side to cancel out as well (negative definite quadratic form). This is equivalent to having $r = h(u)$ and $\kappa(x, u) = 0$.

Since $\dot{\Psi} \leq 0$, we know that the sublevel sets of Ψ are invariant and using Lemma IV.3 we conclude that they are also compact. Therefore, taking $P = \{(x, u) \in \mathbb{R}^{5N} \mid \Psi(x, u) \leq \Psi(x(t_0), u(t_0))\}$ we have that for any initial

condition $(x(t_0), u(t_0))$ the trajectories $(x(t), u(t))$ converge to the largest invariant subset $S \subseteq P$ for which $\dot{\Psi} = 0$.

In particular,

$$\begin{aligned}S &= \{(x, u) \in P \mid \dot{\Psi}(x, u) = 0\} \\ &\subseteq \{(x, u) \in P \mid \|r - h(u)\| = 0, \kappa(x, u) = 0\} \\ &= \{([h(u)^T, \theta]^T, u) \in P \mid \theta \in \mathbb{R}, \nabla\tilde{\Phi}(u) = 0\} \\ &= \{([h(u)^T, \theta]^T, u) \in P \mid \theta \in \mathbb{R}, \nabla\Phi(h(u)) = 0\},\end{aligned}$$

where in the second to last step we used $\nabla\tilde{\Phi}(u) = \kappa(h(u), u)$ and in the last step we used (Assumption III.3),

$$\mathbf{0} = \nabla\tilde{\Phi}(u) = \mathbb{J}h(u)^T \nabla\Phi(h(u)) \iff \nabla\Phi(h(u)) = \mathbf{0}_{2N}.$$

□

In the following we show that we can apply Theorem III.1 to our settings. First, we define

$$W(r, u) = \sum_{i \in \mathcal{V}} W_i(r_i, u_i) = \sum_{i \in \mathcal{V}} \frac{\|r_i - u_i\|^2}{2 \cos(\phi_i(t_0))^2}.$$

Let $\eta_i = \frac{1}{2 \cos(\phi_i(t_0))^2}$, $\alpha = \min_{i \in \mathcal{V}} \eta_i$ and $\beta = \max_{i \in \mathcal{V}} \eta_i$. Then,

$$\alpha \|r - u\|^2 = \min_{i \in \mathcal{V}} \eta_i \sum_{i \in \mathcal{V}} \|r_i - u_i\|^2 \leq W(r, u);$$

$$W(r, u) \leq \max_{i \in \mathcal{V}} \eta_i \sum_{i \in \mathcal{V}} \|r_i - u_i\|^2 = \beta \|r - u\|^2.$$

Using Assumption II.2 to bound $\frac{\cos(\phi_i(t))^2}{\cos(\phi_i(t_0))^2} \leq 1$ we further obtain

$$\begin{aligned}\nabla_r W(r, u)^T \dot{r} &= \sum_{i \in \mathcal{V}} \nabla_{r_i} W_i(r_i, u_i)^T \dot{r}_i = \sum_{i \in \mathcal{V}} \frac{\xi_i \dot{\xi}_i}{\cos(\phi_i(t_0))^2} \\ &= - \sum_{i \in \mathcal{V}} k_i \xi_i^2 \frac{\cos(\phi_i(t))^2}{\cos(\phi_i(t_0))^2} \leq - \sum_{i \in \mathcal{V}} k_i \|r_i - u_i\|^2 \\ &\leq - \min_{i \in \mathcal{V}} k_i \sum_{i \in \mathcal{V}} \|r_i - u_i\|^2 = -\gamma \|r - u\|^2,\end{aligned}$$

with $\gamma = \min_{i \in \mathcal{V}} k_i > 0$.

Then, we observe that $\nabla_{u_i} W_i(r_i, u_i) = \frac{u_i - r_i}{\cos(\phi_i(t_0))^2}$ and thus, we take $\mu = \max_{i \in \mathcal{V}} \mu_i$, with $\mu_i = \cos(\phi_i(t_0))^{-2}$ to obtain

$$\begin{aligned}\|\nabla_u W(r, u)\| &= \sqrt{\sum_{i \in \mathcal{V}} \|\nabla_{u_i} W_i(r_i, u_i)\|^2} \\ &= \sqrt{\sum_{i \in \mathcal{V}} \mu_i^2 \|r_i - u_i\|^2} \\ &\leq \sqrt{\max_{i \in \mathcal{V}} \mu_i^2 \sum_{i \in \mathcal{V}} \|r_i - u_i\|^2} = \mu \|r - u\|.\end{aligned}$$

Therefore, Assumption III.1 with our steady-state input-output map $h(u) = u$ is satisfied. For Assumption III.2 we consider the bound (directly using $\mathbb{J}h(u) = I_{2N}$):

$$\begin{aligned}\|\nabla\Phi(r') - \nabla\Phi(r)\| &= \|(\gamma_1(L_G \otimes I_2) + \gamma_2)(r' - r)\| \\ &\leq \|\gamma_1(L_G \otimes I_2) + \gamma_2\| \|r' - r\|,\end{aligned}$$

so that we can set $l = \|\gamma_1(L_G \otimes I_2) + \gamma_2\|$.

Recalling that $h(u) = u$, Assumption III.3 is trivially satisfied. Finally, our cost function (4) is continuously differentiable with bounded sublevel-sets, because (4b) is a positive definite quadratic form centered in $1 \otimes \tau$ and (4a) is non-negative. Since the pre-image of continuous maps of closed sets (for any c-sublevel set, $[0, c]$ is closed) is closed as well, we can conclude that $\Phi(r)$ has compact sublevel-sets. Therefore, we can apply Theorem III.1 to our robotics coordination problem.

Corollary III.1.1 (Asymptotic convergence). *Assuming that Assumption II.2 holds, the closed-loop system (6) converges asymptotically to the set of critical points of (4) whenever $\epsilon < \sqrt{\frac{\gamma}{\mu l}}$.*

Corollary III.1.2 (Optimality). *The closed-loop system (6) minimises the cost function (4) whenever $\epsilon < \sqrt{\frac{\gamma}{\mu l}}$.*

Proof. To assess the strict convexity of (4) we investigate the second order condition. We derive from (5) $H_\Phi = \gamma_1(L_G \otimes I_2) + \gamma_2$. Using Lemma IV.1 we have that $\lambda \in \text{spec}[\gamma_1 L_G + \gamma_2]$ if and only if $\exists \mu \in \text{spec}[L_G]$ s.t. $(\lambda - \gamma_2)/\gamma_1 = \mu \geq 0$ ([13, Lemma 6.5]) and thus, $\lambda \geq \gamma_2 > 0$. Moreover, by simple permutation of rows we have $\text{spec}[L_G \otimes I_2] = \text{spec}[I_2 \otimes L_G] = \text{spec}[L_G] \cup \text{spec}[L_G]$. Therefore, $H_\Phi \succ 0$ and the critical point u^* s.t. $\nabla \Phi(h(u^*)) = 0$ is unique and attains the minimum of the cost function (4). From Corollary III.1.1 the claim follows. \square

The result of Corollary III.1.2 does not imply that the closed-loop system (6) has a unique equilibrium point. However, it does imply that the set of equilibrium points share the same locations for the agents. Namely, different initial conditions might lead to different final orientations for the agents, as one would intuitively expect.

C. Topological Considerations on the Optimal Configuration

In this subsection, we further investigate the relation between the asymptotic configuration of the swarm and the topology of the formation. Indeed, although Corollary III.1.2 guarantees that the robotics swarm converges to the optimal configuration with respect to (4), it is desirable to know whether the minimisation of the cost function brings the agents into formation around the target location.

In the following, we drop the Kronecker products for ease of notation, and we assume that all the matrices and vectors are comfortably defined. Moreover, we define $r^* = \tau + \delta$ to be the *desirable final configuration*, where δ represents the displacements of the agents from the target location τ when being in the formation defined by d , that is $B^T r^* = d$. It is desirable in the sense that we would like r^* to also minimise the cost (4), which is not the case a priori. Notice that δ is uniquely determined once we fix τ as the centroid of the final configuration $\frac{1}{N} (\sum_{i \in \mathcal{V}} r_i^* = \tau)$ and Assumption II.1 holds. In the following, it is useful to recall $\text{spec}[L_G] = \{0, \lambda_2, \dots, \lambda_N\}$, $0 < \lambda_2 \leq \dots \leq \lambda_N$ [13, Lemma 6.5].

Lemma III.1. *Consider the same setting of Corollary III.1.1. If additionally $\gamma_1 \lambda_2 \gg \gamma_2$ holds, the final configuration $r = h(\bar{u})$, with \bar{u} minimiser of (4), is approximately in the desired formation, namely*

$$\lim_{\gamma_1 \lambda_2 / \gamma_2 \rightarrow \infty} B^T r = d.$$

Proof. Using $0 = \nabla \Phi(r)$ (Corollary III.1.1) and $(\gamma_1 L_G + \gamma_2 I) \succ 0$ (Corollary III.1.2) we have that the final configuration of the agents is

$$r = (\gamma_1 L_G + \gamma_2 I)^{-1} (\gamma_1 B d + \gamma_2 \tau).$$

Using $B d = B B^T r^* = L_G r^*$ and $\tau = r^* - \delta$ we obtain

$$\begin{aligned} r &= (\gamma_1 L_G + \gamma_2 I)^{-1} [(\gamma_1 L_G + \gamma_2 I) r^* - \gamma_2 \delta] \\ &= r^* - (\gamma_1 L_G + \gamma_2 I)^{-1} \gamma_2 \delta. \end{aligned}$$

Since L_G is symmetric, we consider the decomposition $L_G = U \text{diag}([0, \lambda_2, \dots, \lambda_N]) U^T$.

Then (Lemma IV.1, Lemma IV.2),

$$\begin{aligned} &(\gamma_1 L_G + \gamma_2 I)^{-1} \gamma_2 \\ &= U \text{diag}([1, \frac{\gamma_2}{\gamma_1 \lambda_2 + \gamma_2}, \dots, \frac{\gamma_2}{\gamma_1 \lambda_N + \gamma_2}]) U^T \end{aligned}$$

and taking the limit,

$$\lim_{\gamma_1 \lambda_2 / \gamma_2 \rightarrow \infty} (\gamma_1 L_G + \gamma_2 I)^{-1} \gamma_2 = U \text{diag}([1, 0, \dots, 0]) U^T,$$

because $0 < \lambda_2 \leq \dots \leq \lambda_N$ and thus, $\gamma_1 \lambda_i \gg \gamma_2 \forall i \in \mathcal{V}$. Hence, for $\gamma_1 \lambda_2 \gg \gamma_2$, we have

$$(\gamma_1 L_G + \gamma_2 I)^{-1} \gamma_2 \approx U \text{diag}([1, 0, \dots, 0]) U^T.$$

Therefore,

$$\begin{aligned} B^T r &\approx B^T (r^* - U \text{diag}([1, 0, \dots, 0]) U^T \delta) \\ &= B^T r^* - B^T U \text{diag}([1, 0, \dots, 0]) U^T \delta = d. \end{aligned}$$

Therefore, the final configuration is approximately in the desired formation.

In the last equation we use the fact that $B^T U \text{diag}([1, 0, \dots, 0]) U^T = 0$. This can be readily seen as

$$\begin{aligned} &L_G U \text{diag}([1, 0, \dots, 0]) U^T \\ &= U \text{diag}([0, \lambda_2, \dots, \lambda_N]) U^T U \text{diag}([1, 0, \dots, 0]) U^T \\ &= U \text{diag}([0, \lambda_2, \dots, \lambda_N]) \text{diag}([1, 0, \dots, 0]) U^T \\ &= U \text{diag}([0, \dots, 0]) U^T = 0. \end{aligned}$$

Now, let $H = U \text{diag}([1, 0, \dots, 0]) U^T$ and let H_i be the i -th column of H . Then, $\forall i \in \mathcal{V}$, we have that $L_G H_i = 0$. That is, $H_i \in \text{null}[L_G]$. However, $\text{null}[L_G] = \text{null}[B B^T] = \text{null}[B^T]$, where the last step follows from the Finite Rank Lemma [11, Theorem 7.6] with linear map B , adjoint B^T and Hilbert spaces $\mathbb{R}^{|\mathcal{V}|}$ and $\mathbb{R}^{|\mathcal{E}|}$ with the canonical inner product. We have thus obtained that $\forall i \in \mathcal{V}, H_i \in \text{null}[B^T]$. That is, $0 = B^T H = B^T U \text{diag}([1, 0, \dots, 0]) U^T$. \square

Lemma III.1 has a topological interpretation. λ_2 is known as *algebraic connectivity* [13, Definition 6.7] and characterise

the connectivity of the graph [13, Lemma 6.9]. Therefore, a stronger connectivity of the specified formation is expected to result in a final configuration that is approximately the desired one. Moreover, since γ_1 and γ_2 are gains in the gradient-flow (7), they influence the speed of convergence to the formation and the target. Hence, a stronger connectivity of the formation graph allows for a larger γ_2 that in turn allows a faster convergence to the desired location.

Finally, we show that the agents gather in formation around the target. Notice that the problem described by the cost function (4) is not well-posed in the sense that we cannot have both a desired non-trivial formation and all agents in the same target position. Hence, the correctness of the asymptotic behaviour has to be investigated by means of bounds on the distance of the robotics swarm from the target location.

Theorem III.2 (Correct final configuration). *Consider the same settings of Lemma III.1, and let r be the configuration the agents converge to. Then $\|r - \tau\| < \|\delta\|$, with $B^T r \approx d$.*

Proof. From Lemma III.1 we have $r = r^* - (\gamma_1 L_G + \gamma_2 I)^{-1} \gamma_2 \delta$ and thus,

$$\begin{aligned} \|r - \tau\| &= \|r - r^* + \delta\| = \|[I - (\gamma_1 L_G + \gamma_2 I)^{-1} \gamma_2] \delta\| \\ &\leq \|I - (\gamma_1 L_G + \gamma_2 I)^{-1} \gamma_2\| \|\delta\| < \|\delta\|. \end{aligned}$$

Indeed, (Lemma IV.1, Lemma IV.2, [13, Lemma 6.5]), $\forall \mu \in \text{spec}[I - (\gamma_1 L_G + \gamma_2 I)^{-1} \gamma_2]$, there exists $\lambda \in \text{spec}[L_G]$ such that

$$\mu = 1 - \frac{\gamma_2}{\gamma_1 \lambda + \gamma_2} = \frac{\gamma_1 \lambda}{\gamma_1 \lambda + \gamma_2} \in [0, 1),$$

and thus, $\|I - (\gamma_1 L_G + \gamma_2 I)^{-1} \gamma_2\| < 1$. Finally, $B^T r \approx d$ is immediate from Lemma III.1. \square

As one would intuitively expect, the formation shrinks around the target due to the attractive force. However, in the limit $\gamma_1 \lambda_2 \gg \gamma_2$ we achieve the correct inter-agent distances.

IV. PROOFS

A. Proof of Lemma II.1

In the following we drop the indices for convenience.

Proof. First, we observe that

$$\dot{\xi} = \frac{-(p - r)^T}{\|p - r\|} \dot{r} = -\frac{\xi_a v \cos(\theta) + \xi_b v \sin(\theta)}{\xi} \quad (9)$$

$$\begin{aligned} &= -v \cos(\phi) \\ \dot{\phi} &= \frac{v}{\xi} \sin(\phi) - \omega, \end{aligned} \quad (10)$$

where we use the identities $\cos(\alpha + \beta) = \cos(\alpha) \cos(\beta) - \sin(\alpha) \sin(\beta)$, $\sin(\alpha + \beta) = \sin(\alpha) \cos(\beta) + \sin(\beta) \cos(\alpha)$ and notice that $\cos(\text{atan2}(b, a)) = a/\sqrt{a^2 + b^2}$ and $\sin(\text{atan2}(b, a)) = b/\sqrt{a^2 + b^2}$.

Substituting the proposed control law we obtain

$$\dot{\xi} = -k \xi \cos(\phi)^2, \text{ and } \dot{\phi} = -k \frac{\sin \phi^2}{\phi}.$$

Notice that $\dot{\phi}$ can be extended by continuity at $\phi = 0$ with $\dot{\phi} = 0$, i.e., $\phi = 0$ is an equilibrium point for ϕ . Hence, we can invoke the Peano-Cauchy existence theorem to guarantee that a solution trajectory exists. Furthermore, the proposed control law decouples ϕ from ξ .

We now consider the Lyapunov function $V_\phi(\phi) = \frac{1}{2} \phi^2$, which is radially unbounded and positive definite.

We have that $\dot{V}_\phi(\phi) = \phi \dot{\phi} = -k \sin \phi^2 \leq 0$. Therefore, $\phi = 0$ is stable [13, Theorem 15.4].

Notice that $\dot{V}_\phi(\phi) = 0$ if and only if $\phi = n\pi, n \in \mathbb{Z}$. If $|\phi(t_0)| < \pi/2$, then we have asymptotic stability of $\phi = 0$ [13, Theorem 15.4], because $|\phi(t)| \leq |\phi(t_0)|$ from the invariance of the sublevel sets of V_ϕ . Moreover, we have also $\cos(\phi(t)) \geq \cos(\phi(t_0))$.

Since there exist $\phi(t)$, we now know that $\dot{\xi}$ is of the form $f(\xi, t)$, Lipschitz in its first argument and continuous in its second one. Therefore, from the theorem of existence and uniqueness [14, Theorem 3.2], we claim that there exist a unique solution $\xi(t)$ for any initial $\xi(t_0) \geq 0$.

In particular, the solution is of the form

$$\xi(t) = \xi(t_0) \exp\left(-k \int_{t_0}^t \cos(\phi(s))^2 ds\right).$$

Recalling that $\cos(\phi(s))^2 = 1 - \sin(\phi(s))^2$ and noticing that $\sin(\phi(s))^2 = \phi(s)\phi(s)$, integrating by parts we obtain

$$\int_{t_0}^t \cos(\phi(s))^2 ds = t - \frac{\phi(t)^2 - \phi(t_0)^2}{2}.$$

Since $\phi(t)^2 \leq \phi(t_0)^2$, we have $\xi(t) \leq \xi(t_0) \exp(-kt)$, i.e., $\xi = 0$ is a globally exponentially stable equilibrium. \square

B. On the eigenvalues of related matrices

In the following we consider $M \in \mathbb{R}^{n \times n}$, with eigenvalues $\text{spec}[M] = \{\lambda_1, \dots, \lambda_n\}$.

Lemma IV.1. $\text{spec}[\alpha M + \beta] = \{\alpha \lambda_1 + \beta, \dots, \alpha \lambda_n + \beta\}$.

Proof. We have that $0 = \det[\mu I - (\alpha M + \beta)]$ if and only if $0 = \det[\frac{\mu - \beta}{\alpha} I - M]$. Therefore, $\mu \in \text{spec}[\alpha M + \beta] \iff \frac{\mu - \beta}{\alpha} \in \text{spec}[M]$. Applying the inverse transformation we obtain the claim. \square

Lemma IV.2. If $\exists M^{-1}$, $\text{spec}[M^{-1}] = \{\lambda_1^{-1}, \dots, \lambda_n^{-1}\}$.

Proof. Let v be an eigenvector associated to the eigenvalue λ of M . Since $\exists M^{-1}$, $0 \notin \text{spec}[M^{-1}]$. Then $v = M^{-1} M v = \lambda M^{-1} v$ if and only if $M^{-1} v = \frac{1}{\lambda} v$, which completes the proof. \square

C. Steady state input output map

From the definition of the steady-state input-output map h of the i -agent, we set $f([h_i(u_i)^T, \theta_i]^T, u_i) \stackrel{!}{=} 0$. Hence,

$$\begin{cases} 0 \stackrel{!}{=} v_i \cos(\theta_i) \\ 0 \stackrel{!}{=} v_i \sin(\theta_i) \end{cases} \iff 0 = v_i = \|u_i - h_i(u_i)\|$$

That is, $u_i = h_i(u_i)$. Given Lemma II.1, Assumption II.2 and stacking the maps of the single agents we obtain $h(u) = u$.

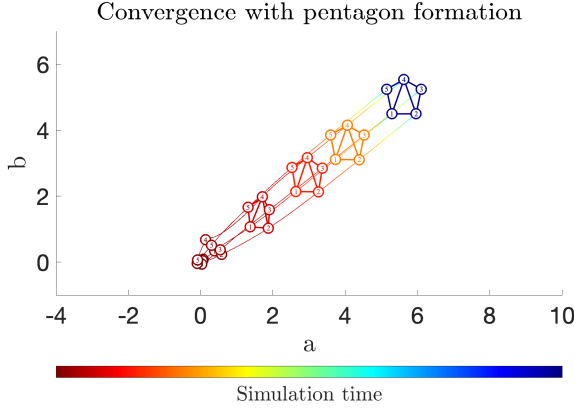


Fig. 3. Evolution over time of a swarm of 5 agents in the $a - b$ plane. They start from random positions around the origin and they converge to the specified pentagon formation around the target location $\tau = [5.65, 5.03]^T$. The time evolution is colour-coded from red (beginning) to blue (end).

D. On the compactness of sublevel sets

We now provide a simple extension to [10, Lemma A.2].

Lemma IV.3. *Consider a stable system (6a) satisfying Assumption III.1 and Assumption III.3. Let $g(x)$ be the measured portion of the state and $Z(x, u) = V(u) + W(g(x), u)$, where V is a continuous positive-semidefinite function with compact sublevel sets, and W is the function defined in Assumption III.1. Then, the sublevel sets of Z are compact.*

Proof. Let $\Omega_c = \{(x, u) | Z(x, u) \leq c\}$ be a sublevel set of Z . $W \geq 0$ implies $V \leq c$, and since V has compact sublevel sets, $\|u\| \leq U$ for some U . Similarly, $W \leq c$ since $V \geq 0$. Let $r = g(x)$ be the measured state, and \bar{r} the unmeasured, stable, portion. Notice that the stability of \bar{r} implies that for any initial condition $x(t_0)$ there exists B such that $\|\bar{r}\| \leq B$. From Assumption III.1 we have $\|r - h(u)\| \leq \frac{1}{\alpha} W(x, u) \leq \frac{c}{\alpha}$, and thus,

$$\begin{aligned} \|x\| &\leq \|\bar{r}\| + \|r\| \\ &\leq \|\bar{r}\| + \|r - h(u)\| + \|h(u) - h(0)\| + \|h(0)\| \\ &\leq \|\bar{r}\| + \frac{c}{\alpha} + q\|u\| + \|h(0)\| \\ &\leq B + \frac{c}{\alpha} + qU + \|h(0)\|, \end{aligned}$$

where q is the Lipschitz constant of h (Assumption III.3). Therefore, we can conclude that $\|x\|$ is bounded and thus, $\|(x, u)\|$ is bounded for all $(x, u) \in \Omega_c$. The continuity of V and W (and thus, Z) allows us to conclude that Ω_c is also closed. Indeed, the pre-image of a continuous map on a closed set (such as $[0, c]$) is closed. \square

V. EXAMPLES AND EMPIRICAL RESULTS

In this section, we provide simulation examples to underline the transient behaviour under the provided cost function (4), and we show what can go wrong when the assumptions of Theorem III.2 fail. The MATLAB code for the simulations is available on GITHUB.

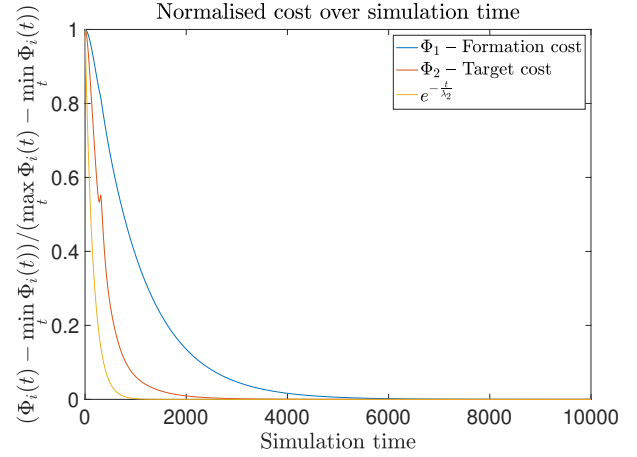


Fig. 4. (Normalised) terms $\Phi_1(4a)$, $\Phi_2(4b)$, formation and target cost respectively, of the objective function (4) over time for the pentagon formation (Figure 3). The evolution resembles an exponential decay, $(\exp(-t/\lambda_2))$ is juxtaposed for comparison purposes.

In Figure 3 a simulation for a swarm of 5 agents is shown. The pentagon formation is specified by

$$B = \begin{bmatrix} 1 & 0 & 0 & 0 & -1 & 1 & 0 \\ -1 & 1 & 0 & 0 & 0 & 0 & -1 \\ 0 & -1 & 1 & 0 & 0 & 0 & 0 \\ 0 & 0 & -1 & 1 & 0 & -1 & 1 \\ 0 & 0 & 0 & -1 & 1 & 0 & 0 \end{bmatrix}$$

and the relative position vector (reshaped in a $2 \times N$ matrix for readability reasons) is

$$d = \begin{bmatrix} -1.0 & -0.3 & 0.8 & 0.8 & -0.3 & -0.5 & -0.5 \\ 0.0 & -1.0 & -0.3 & 0.3 & 1.0 & -1.3 & 1.3 \end{bmatrix}.$$

The agents start from random positions in a neighbourhood around the origin, they assemble in formation and move together towards the specified target location. In Figure 3, one can appreciate the time evolution visualized by the change in colour. It is apparent that the specified cost function guarantees that the agents do not only drive to the target location before assembling in formation, but they do so early on. Hence, the desired transient behaviour is empirically obtained. Characterising it quantitatively is still an open question and a topic of ongoing research. In Figure 4 the evolution over time of the two terms of the cost function (4) is shown. The resemblance to an exponential decrease is apparent from the juxtaposition with e^{-t/λ_2} , λ_2 being the algebraic connectivity of the specified pentagon formation. Indeed, we intuitively expect the decrease rate to be somehow related to the gains of the cost function and the algebraic connectivity of the formation graph.

Next, we consider an E-shaped formation, which is clearly not circularly symmetric around its centroid and thus, the cost term (4b) will shrink and distort the formation for poorly chosen gains. In Figure 5 and Figure 6 the simulations of the robotics swarm with different values for the gains γ_1 and γ_2 are shown. It is apparent that when the conditions of Theorem III.2 are not fulfilled, the final configuration of the

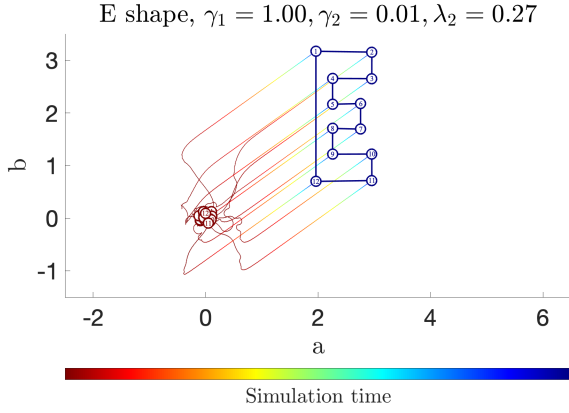


Fig. 5. Evolution over time of a swarm of 12 agents in the $a-b$ plane. The robots converge to the desired formation and location asymptotically, since the conditions of Theorem III.2 hold. The time evolution is colour-coded from red (beginning) to blue (end).

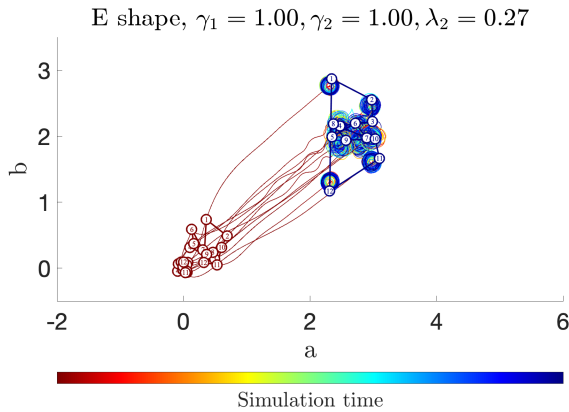


Fig. 6. Evolution over time of a swarm of 12 agents in the $a-b$ plane. Oppositely to Figure 5, the conditions of Theorem III.2 do not hold and thus, the final configuration is not the desired one. That is, the cost function does not capture the desired goal of the task. The time evolution is colour-coded from red (beginning) to blue (end).

agents is not the desired one (Figure 6). On the other hand, we empirically notice that a factor of 10 between $\gamma_1 \lambda_2$ and γ_2 is enough to obtain the desired result in Figure 5.

VI. CONCLUSIONS AND FUTURE WORK

In this article, we applied feedback optimisation to guide a swarm of agents towards a target location while self-sorting in formation. We showed that the resulting control law is distributed and we provided conditions under which the agents achieve asymptotic convergence to the optimal configuration for the designed cost function. Lastly, we derived a topological criterion on the specified formation to quantitatively guarantee that the final configuration is indeed close to the desired one.

To conclude, we want to outline some possible directions for further work on the topic. First, being able to prove

the optimality of the final configuration in presence of non-convexities due to obstacle avoidance terms or visibility constraints would represent a natural extension to the work presented in this paper. Additionally, another interesting venue of research would be to quantify to what extent feedback optimisation implicitly deals with noisy dynamics and input saturation. Finally, quantitatively characterising the transient behaviour of the closed loop system is still a major question to address in the context of feedback optimisation.

REFERENCES

- [1] Adrian Hauswirth et al. “Optimization Algorithms as Robust Feedback Controllers”. In: (2021).
- [2] Jing Wang and Nicola Elia. “A control perspective for centralized and distributed convex optimization”. In: *2011 50th IEEE Conference on Decision and Control and European Control Conference*. 2011, pp. 3800–3805.
- [3] Daniel K Molzahn et al. “A Survey of Distributed Optimization and Control Algorithms for Electric Power Systems”. In: *IEEE Transactions on Smart Grid* 8.6 (2017), pp. 2941–2962.
- [4] Lukas Ortmann et al. “Experimental validation of feedback optimization in power distribution grids”. In: *Electric Power Systems Research* 189 (Dec. 2020), p. 106782.
- [5] Chin Yao Chang et al. “Saddle-Flow Dynamics for Distributed Feedback-Based Optimization”. In: *IEEE Control Systems Letters* 3.4 (Oct. 2019), pp. 948–953.
- [6] Adrian Hauswirth et al. “Time-varying Projected Dynamical Systems with Applications to Feedback Optimization of Power Systems”. In: *2018 IEEE Conference on Decision and Control (CDC)*. 2018, pp. 3258–3263.
- [7] Craig W Reynolds. “Flocks, Herds and Schools: A Distributed Behavioral Model”. In: *Proceedings of the 14th Annual Conference on Computer Graphics and Interactive Techniques*. SIGGRAPH ’87. New York, NY, USA: Association for Computing Machinery, 1987, pp. 25–34.
- [8] R Olfati-Saber. “Flocking for multi-agent dynamic systems: algorithms and theory”. In: *IEEE Transactions on Automatic Control* 51 (2006), pp. 401–420.
- [9] Giuseppe Belgioioso et al. “Sampled-Data Online Feedback Equilibrium Seeking: Stability and Tracking”. In: (Mar. 2021).
- [10] Adrian Hauswirth et al. “Timescale Separation in Autonomous Optimization”. In: (2019).
- [11] John Lygeros and Federico Alessandro Ramponi. “Lecture Notes on Linear System Theory”. In: (2015).
- [12] Petar Kokotović, Hassan K. Khalil, and John O’Reilly. “7. Nonlinear Systems”. In: *Singular Perturbation Methods in Control: Analysis and Design*, pp. 289–337.
- [13] Francesco Bullo. *Lectures on Network Systems*. 2020.
- [14] Hassan K Khalil. *Nonlinear systems*. 3rd ed. 2002.